TRANSITION FROM LAMINAR TO NON-DARCY FLOW OF GASES IN POROUS MEDIA

Rashed Noman* and **M. Zubair Kalam****
BP Research, Sunbury-on-Thames, UK
* now with Texaco Ltd, UK
** now with University of Oman

Abstract Experimental investigation has been carried out to examine critical velocities at which transition from laminar to non-Darcy flow of gases take place. The critical velocities were evaluated from back-pressure plots of pressure gradient against flow rates. Incorporating the gas slippage effects into these plots resulted in significantly higher critical velocities. The critical velocities were found to be related petrophysically to the permeability, porosity and pore structure of the sample.

INTRODUCTION

Determination of the critical velocity at which gases flowing through a porous medium start to deviate from Darcy's law is of interest to core analysis as well as gas reservoir engineering. During fluid flow through narrow pipes or capillaries, it is well known that a very rapid transition from laminar to turbulent flow can occur depending on the Reynolds number of the flow ($Re = \rho vd/\mu$). The critical value is generally accepted to be around $Re = 2000$. It would be useful to find such a critical Reynolds number for flow in porous media, eg. in the interpretation of experimental flow data or to estimate the region where non-Darcy effects would become significant in high rate gas wells. The purpose of this work is to provide a method by which this transition rate could be estimated.

FLOW REGIMES

Due to the wide distribution of pore sizes and shapes in any naturally occuring porous medium, it is possible for two more different modes of flow to coexist simultaneously. The difficulty of describing the transition rates between two modes of flow is therefore obvious. It is nevertheless possible to divide flow in porous media into a number of broad catagories. This is not a matter of semantics alone, since a different mathematical expression may be required for the best description of each mode of flow. Some of the various types of flow in porous media and the equations used to described them are:

(a) diffusional flow (Knudsen equation)
(b) molecular slip flow (Klinkenberg equation)
(c) viscous flow (Darcy's law)
(d) visco-inertial flow (a transition region)
(e) inertial dominated flow (Forchheimer equation)
(f) inertial/turbulence transitional region
(g) turbulent flow (a cubic equation)

There are many other types of flow where Darcy's law would be inapplicable. These will however not be discussed here (see Scheidegger, 1974; Bear, 1972). The present study will focus on the transition from viscous (linear) to inertial dominated (non-linear) flow, usually known as the 'non-Darcy' flow region.

Experimental observation using laser doppler anemometry (Dybbs et al, 1984) on porous media consisting of glass bead packs has shown that in the Darcy regime, where the flow is dominated by viscous forces, the exact nature of the flow is determined by the local geometry of pore spaces. This type of flow has been found to be valid for $Re<1$, where the value of Re was based on average pore size and the average pore velocity. At $Re=1$, boundary layers were found to develop near the solid boundaries of the pore. A transition region was found to occur at Re between 1 and 10 where the flow changed from purely viscous to inertial dominated. Here the boundary layers became more pronounced and an "inertial core" appeared. The developement of these "core" flow outside the boundary layers was found to be the cause for a nonlinear relationship between the pressure gradient and the flow rate. This nonlinear flow relationship persisted to a Re of 200. Flow in the range $200<Re<350$ was of an unsteady laminar type, which was characterised by laminar wake oscillations in the region $200<Re<300$ and was followed by the formation of vortices in the range $300<Re<350$. Thereafter, at $Re>350$, a highly unsteady and chaotic flow pattern ensued which resembled turbulent flow.

It is important to remember that for consolidated porous media, the transitional flow rates may be quite different due to the complexity and heterogeneity of the pore structure. The general trend of flow regimes as described above would however be expected to hold for many types of porous media.

THEORY

The permeability of a porous medium is evaluated from the definition of Darcy's law. For flow of gases, since the volumetric flow rate varies with pressure, it is necessary to use either an integrated form of the equation or alternatively an average value of the flow rate. If an average pressure is used, the volume at mean pressure has to be converted to a volume measured at one atmosphere, so that Darcy's law may be expressed as

$$Q = KA(P_1^2 - P_2^2)/2\mu Z P_o L \tag{1}$$

where P_o is the reference pressure and P_1, P_2 are the upstream and downstream pressures. This equation however cannot be used to determine the permeability of porous media using gas. This is because gas molecules are affected by the 'slippage' effect, as the mean free path of the molecules approach the dimension of the pore openings. From consideration of gas flow through straight capillaries, Klinkenberg (1941) showed that the permeability of gas could be expressed as :

$$K_a = K_l \ (1+4c\lambda/r) \tag{2}$$

where c is a constant. Since the mean free path, λ, is inversely proportional to P, and r, a characteristic length scale describing the medium, is a constant, Equation (2) could be rewritten as :

$$K_a = K_l \ (1+b/P_m) \tag{3}$$

Equation (3) shows that if the apparent permeability, K_a, is plotted against the inverse of mean pressure, P_m, a straight line can be obtained, the intercept of which will give the true gas permeability and is eqivalent to the permeability K_l which would be obtained by flowing a liquid through the medium. The intercept is essentially an extrapolation of the apparent permeabilities to an infinite mean pressure.

As the gas flow rate is increased in a core sample, deviation from Darcy's law begin to take place due to inertial forces becoming more dominant than the viscous forces. An equation for describing flow at the inertial dominated regime was first proposed by Forchheimer (1901), and can be written as:

$$-\nabla P = \alpha \ \mu \ v + \beta \ \rho \ v^2 \tag{4}$$

where α is the viscous resistance coefficient, and is eqivalent to the inverse of permeability at low flow rates (ie. Darcy's law), and β is the inertial resistance coefficient. The viscous and inertial coefficients are independent of the fluid properties and depend only on the nature of the porous medium.

In the Forchheimer equation, the first term represents the pressure drop due to the viscous forces and the second term that due to inertial forces. Since Reynolds number is the ratio of the inertial to viscous forces, it was suggested (Green et al, 1951) that the Reynolds number for a porous medium could be represented by

$$Re = \rho v(\beta/\alpha)/\mu \tag{5}$$

The characteristic length scale of the porous media is therefore represented by the term β/α, ie. βK. This definition has been used widely in the literature (Geertsma, 1974; Ahmed et al, 1969; Wright, 1968, etc). The present experimental work suggest that this definition may be incorrect for representing the characteristic length scale, as will be discussed below.

An alternative to using the Reynolds number is to use the Darcy's law directly to determine the flow rate for the onset of deviation. Since the absolute permeability for a porous medium is a constant and μZ is approximately constant for the low pressures used in most experiments, then, according to Equation (1) a plot of the pressure drop squared against flow rate should yield a straight line passing through the origin. Any deviation from this line will indicate a departure from Darcy's law. The flow rate at which this departure will occur can be expected to be a unique value dependent on the pore structure of the media and the fluid used. A typical plot of pressure drop against flow rate is shown in Figure 3. The plot confirms our expectation and a departure from the straight line is observed as the flow rate increases. Comparison of the flow rate at which departure occurs with the Klinkenberg plots (Figure 1) for the same sample, it was found that the departure from the straight line occured much earlier than was expected. It was then realised that Darcy's law as expressed in Equation (1) should not be used directly since the permeability is actually not the absolute one but an apparant value affected by slippage at low pressures. It is possible to account for this slippage (Dranchuk et al, 1969) by substituting the Klinkenberg equation into the Darcy's equation, which then becomes

$$Q = \frac{KA}{2\mu Z P_o L} (1+b/P_m)\,(P_1{}^2-P_2{}^2) \qquad (6)$$

The permeability in the above equation is now the absolute value and is equivalent to the liquid permeability, K_1. According to this modified form of Darcy's law, a plot of $(1+b/P_m)(P_1{}^2-P_2{}^2)$ against the flow rate would yield a straight line passing through the origin since all other terms in the equation remain constant. This is indeed found to be the case, as shown in Figure 4. Departure from the straight line occurs at increasingly higher flow rates.

EXPERIMENTAL

Porosity of 23 core plugs aquired from a number of wells in the North Sea area were measured using the helium gas expansion technique.

Permeability of these samples were measured by flowing air at various flow rates and plotting the data according to Klinkenberg's formula. The slippage "correction factors", b, in

Equation (3), were calculated from the slope of the Klinkenberg plots. A typical plot is shown in Figure 1.

The inertial coefficient, β, was calculated by plotting the flow data according to an intergrated form of the Forchheimer equation (Dranchuk et al, 1968) which may be expressed as

$$\frac{(P_1^2-P_2^2)M}{2ZRT\mu L(W/A)} = \frac{W\beta}{A\mu} + \frac{1}{K} \tag{7}$$

By plotting the left hand side against $(W/A\mu)$ the value of β could be obtained as the gradient of the slope. A typical plot is shown in Figure 2. Results of these measurement are shown in Table 1.

The results of the flow tests were plotted according to Darcy's law for gas, ie. pressure drop squared against flow rate. One such plot is shown in Figure 3. The flow data with pressure gradients modified to take account of slippage (Equation 6) were also plotted; an example of this is shown in Figure 2. The onset of deviation from Darcy's law was estimated from these plots in both cases and are reported in Table 1. The final column in Table 1 is the flow rate at the onset of deviation per unit cross sectional area (in cm/sec).

DISCUSSION

In both the Klinkenberg and Forchheimer type of plots, the data points show a downward warp (see Figures 1 and 2). In the former, this is due to inertial effect becoming significant at high flow rates and in the latter this is due to gas slippage effect becoming important at the lower flow rates. In the case of Klinkenberg plots it may be necessary to impose some back pressure while being able to vary the mean pressure to be able to obtain a straight line. Otherwise inertial effects may start to become significant and a straight line drawn through any set of data points will give erroneous results. In the case of Forchheimer plots, it is necessary to have a sufficiently high flow rate (and mean pressure) to minimise gas slippage effects.

If the deviation from Darcy's law is assumed to take place at a Reynolds number of one (as is generally assumed in the literature), then the critical flow rate for deviation from Darcy's law can be predicted directly from the definition of Reynolds number. Equation (5) could then be rewritten as:

$$v = A\phi\mu/\rho d \tag{8}$$

where

$$d = \beta K$$

The porosity term ϕ is introduced to ensure that the Reynolds number is based on the interstitial velocity of the fluid and not calculated assuming that the flow takes place across the whole cross section of the sample, as is often done in the literature.

The observed critical velocities are shown in Table 2 along with those calculated using the above equation, ie. assuming that the transition occurs at a Re=1. The calculated critical flow velocities are generally found to be much larger than the experimentally observed values - sometimes by as much as two orders of magnitude. The difference between the observed and the calculated values generally increase as the permeability of the sample decrease. These results suggest that for rocks of moderate permeability (10-100 md) the critical Reynolds number, as defined in Equation (5), could indeed be around 1. For rocks of lower permeability (1-10 md) the critical Re would be around 0.1, and for rocks with permeability in the range 0.1-1 md, the critical Re is likely to be around 0.05. The Reynolds number as calculated from the experimentally determined critical velocities (using Equation 5) are shown in the final column of Table 2 for comparision. It should be noted that as permeability decreases, the pore structure also tend to become more complicated, eg. due to the growth of authigenic clays. This therefore helps to bring the nonlinear mode of flow much earlier than for high permeability samples.

At a given scale of observation it is reasonable to expect that as the permeability of a rock sample increases, so its mean pore size will also increase. The characteristic length parameter, d ($=\beta/\alpha$) in the Reynolds number, as defined by Green et al (1951) should therefore become larger with increasing permeability. Values of d were calculated for a number of samples and plotted against their permeability to verify this assumption (Figure 5). Although the data has a wide scatter, the trend is obviously downwards. The plot shows that the characteristic length, d, decreases with increasing permeability, which is contrary to expectation. This therefore brings into question the validity of using the definition proposed by Green et al (1951). The above discussion shows that there is no simple or unique way of defining a suitable length parameter which will characterise a porous medium and could be used in the Reynolds number. It therefore seems that the best way of finding the transitional flow rate is to plot the flow data according to Equation (6).

Comparision of plots according to Equations (1) and (6) showed that the delay in the onset of deviation from a straight line was generally much higher for lower permeability plugs - sometimes by as much as 20 times. For high permeability samples this may not be very significant. For instance, in a core plug of permeability about 100 md, inclusion of the slippage correction term changed the critical flow by only about 5%. This seems to be reasonable since slippage is more prominent in low permeability core samples.

Using the modified pressure gradient against flow rate plots, the onset of deviation from Darcy's law was found for the core plugs and are reported in Table 1. It was found that the flow rates at the onset of deviation from Darcy's law could be correlated to the permeability of the rock sample. A plot of the critical flow rates versus permeability is shown in Figure 6 . The scatter in the data shows that in addition to permeability, there are other pore structural parameters causing the transition from laminar to non-Darcy flow to occur. The plot suggests that the critical flow velocity is a unique value for the medium and for the particular fluid used. It was possible to obtain a better correlation when the critical flow velocities were plotted against $\sqrt{(k/\phi)}$, as shown in Figure 7, since this parameter provides a better characterisation of the pore structure.

There is a considerable amount of evidence in the literature to suggest that the critical velocity for transition is strongly dependent on the pore structure of the media (Houpert, 1959). Fancher et al (1933) for instance, studied the deviation from Darcy's law at high rates by a series of systematic experiments and found that for unconsolidated sands, a plot of the Fanning Friction factor against Reynolds number (using the grain size) can be used to draw a single line for all data points. However for consolidated media, a definite line was observed for each media. They explained that this was due to the size and shape of pores in a consolidated medium, and also due to the amount and arrangement of cementing materials and the degree of angularity of sand grains. Of these they found from experiments that the amount and arrangement of cementing materials was the most significant.

Others have carried out experiments using glass bead packs to observe the transition from laminar to fully turbulent flow. McFarland et al (1976) used packs with bead diameters of 0.25 and 0.5 inches and the packing arrangements of cubic and orthorhombic type. Their results show that the Reynolds number (based on grain size) for the transition to turbulence changes 10 folds if the packing arrangement is changed and by 20 folds if the diameter is also changed. Blick (1966) has also carried out experimental work and suggests that the slight discrepency between his proposed theory and his experimental observations is due to the way in which mean pore diameter is defined and measured. He suggests that incorporation of pore size distribution data from capillary pressure curves might be the path to an improved description. Various researchers have also attempted to incorporate 'shape factors' for describing flow through porous media. These shape factors however have to be determined empirically.

CONCLUSIONS

It has not been possible to adequately describe the transition from laminar flow to inertial dominated flow by the use of Reynolds number. This is because the Reynolds number requires a characteristic length parameter, which cannot be described accurately due to the difficulty of quantifying the pore structure in naturally occuring porous media. Conventional definition of the characteristic length using (β/α) may be incorrect since current experimental results show that it decreases with increasing permeability.

To able to define the onset of non-Darcy flow it is necessary to carry out flow measurements on the core material of interest and to plot the data according to Equation (6). This equation is a modified form of the Darcy's law which takes into account the gas slippage effect. Critical gas velocities can be found from the onset of deviation from a straight line according to this type of plot. Critical velocity measured in this manner is found to be a unique function of the medium, and is dependent on its porosity, permeability and the pore structure.

It was possible to obtain a very good correlation between the critical velocity and the permeability of the core samples investigated in this study. An improvement in the correlation could be obtained between the critical velocities and the parameter $\sqrt{(k/\phi)}$.

ACKNOWLEDGEMENT

The authors would like to thank the management of BP for permission to publish this work.

NOMENCLATURE

A = cross-sectional area, L^2
d = characteristic length in Reynolds number, L
k = permeability, L^2
L = length of the core sample, L
M = molecular weight of gas
P = pressure, M/LT^2
Q = volumetric flow rate, L^3/T
R = universal gas constant
T = absolute temperature
v = fluid velocity, L/T
W = mass flow rate, M/T
Z = gas compressibility factor
α = coefficient of viscous flow resistance, $1/L^2$
β = coefficient of inertial flow resistance, 1/L
ρ = density, M/L^3
ϕ = porosity
μ = gas viscosity, M/LT

REFERENCES

AHMED, N. and SUNADA, D.K. (1969) Non-linear flow in porous media. J. Hydraulics, Proc ASCE, 95, 1847.

BEAR, J. (1972) Dynamics of Fluids in Porous Media, American Elsevier, New York.

BLICK, E.F. (1966) Capillary orifice model for high speed flow through porous media. Ind. Eng. Chem., 5, 90-94.

DRANCHUK, P.M. and KOLADA, L.J. (1968) Interpretation of steady linear visco-inertial gas flow data. J. Can. Pet. Tech., Jan., pp.36-40.

DYBBS, A. and EDWARDS, R.V. (1984) A new look at porous media fluid mechanics - Darcy to turbulent. in Fundamentals of Transport in Porous Media (Ed.: J.Bear) Martinus Nijhoff, Series E, No.82, pp 201-256.

FANCHER, G.H. and LEWIS, J.A. (1933) Flow of simple fluids through porous materials. Ind. Eng. Chem., 25(10), 1139.

FORCHHEIMER, P. (1901) Wasserbewegung durch Boden. Z. Ver. Duetsch. Ing., 45, 1782-88.

GEERTSMA, J. (1974) Estimating the coefficient of inertial resistance in fluid flow through porous media. Soc. Pet. Eng. J., Oct, 445.

GREEN, L. and DUWEZ, P.J. (1951) Fluid flow through porous metals. J. Appl. Mech., 18, 39.

HOUPERT, A. (1959) On the flow of gases in porous media. Revue L'Inst. Francaise Petrole, 14, 1468.

KLINKENBERG, L.J. (1941) The permeability of porous media to liquids and gases. Drill. Prod. Prac., A.P.I., pp. 200.

McFARLAND, J.D. and DRANCHUK,P.M. (1976) Visualisation of the transition to turbulent flow in porous media, J. Can. Pet. Tech., April, 71-78.

SCHEIDEGGER, A.J. (1974) The physics of flow through porous media. Toronto Univ. Press, Toronto.

WARD, J.C. (1964) Turbulent flow in porous media. J. Hydraulics, Proc. ASCE, Sept, 1-12.

WRIGHT, D.E. (1968) Nonlinear flow through granular media. J. Hydraulics, Proc ASCE, July, 851-872.

TABLE 1

Flow rate data

Sample	k (md)	ϕ (%)	β k (μm)	√ k/ϕ (md)	Flow rate (cc/s)	Modified (cc/s)	Velocity (cm/s)
M11001	59.0	20.76	71.23	16.86	3.5	17.0	3.41
M11002	2.18	13.82	1080.	3.97	0.35	3.2	0.64
M11005	0.98	10.19	4210.	3.10	0.15	1.0	0.20
M11008	1.23	12.74	972.	3.11	0.3	0.6	0.12
LE253	0.41	7.43	106.6	2.35	0.16	0.65	0.13
LE718	0.041	6.83	382.6	0.77	0.042	0.065	0.013
LE728	0.26	11.39	722.3	1.51	0.14	0.35	0.07
RH94	2.21	12.17	125.4	4.26	0.19	1.4	0.28
RH97	17	16.92	112.7	10.02	1.10	5.0	1.0
RH99	5.9	14.90	142.8	6.29	0.80	3.5	0.70
RH101	0.14	5.87	3642.4	1.54	0.03	0.07	0.014
RH103	0.23	9.96	852.7	1.52	0.052	0.40	0.08
M73001	0.064	12.31	9010	0.71	0.01	0.10	0.02
M73002	0.10	11.50	5880	0.94	0.015	0.11	0.02
M73003	0.46	10.01	1320	2.14	0.025	0.30	0.06
M73004	0.51	11.0	1240	2.16	0.03	0.65	0.13
M73005	33.0	21.0	56.7	12.54	0.55	10.0	2.0
M73006	15.2	20.5	58.9	8.61	0.35	9.0	1.8
M73007	10.5	20.9	69.9	7.09	0.25	4.0	0.8
M73008	13.0	23.9	46.5	7.37	0.5	8.5	1.7
M73009	32.5	25.6	28.4	11.27	0.95	15.0	3.0
M73012	28.4	19.6	59.9	12.04	0.90	8.5	1.7
M73013	20.8	19.01	56.2	10.46	0.45	8.0	1.6

TABLE 2

Reynolds number at critical velocities

Sample	permeability (md)	Critical Velocities (cm/s) observed	Critical Velocities (cm/s) calculated @ Re = 1	Re
M11001	59.0	3.41	8.57	0.40
M11002	2.18	0.64	0.56	1.14
M11005	0.98	0.20	0.14	1.43
M11008	1.23	0.12	0.63	0.19
LE253	0.41	0.13	5.73	0.023
LE718	0.041	0.013	1.60	.0081
LE728	0.26	0.07	0.85	0.083
RH94	2.21	0.28	4.87	0.057
RH97	17.0	1.0	5.42	0.18
RH99	5.9	0.70	4.28	0.16
RH101	0.14	0.014	0.17	0.083
RH103	0.23	0.08	0.72	0.11
M73001	0.064	0.02	0.068	0.29
M73002	0.012	0.02	0.10	0.19
M73003	0.46	0.06	0.46	0.13
M73004	0.51	0.13	0.49	0.26
M73005	33.0	2.0	10.77	0.19
M73006	15.2	1.8	10.37	0.17
M73007	10.5	0.8	8.74	0.09
M73008	13.0	1.7	13.13	0.13
M73009	32.5	3.0	21.50	0.14
M73012	28.4	1.7	10.19	0.17
M73013	13.0	1.6	10.87	0.15

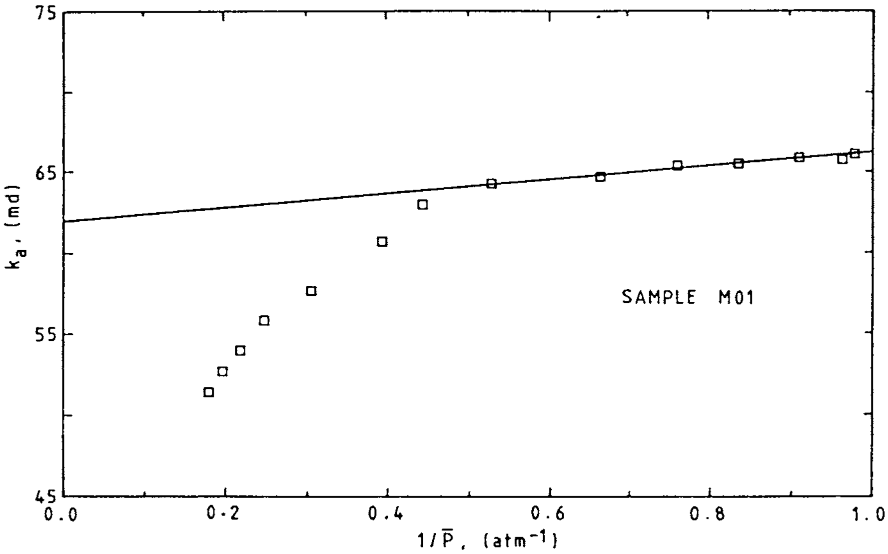

Fig. 1 An example of Klinkenberg plot

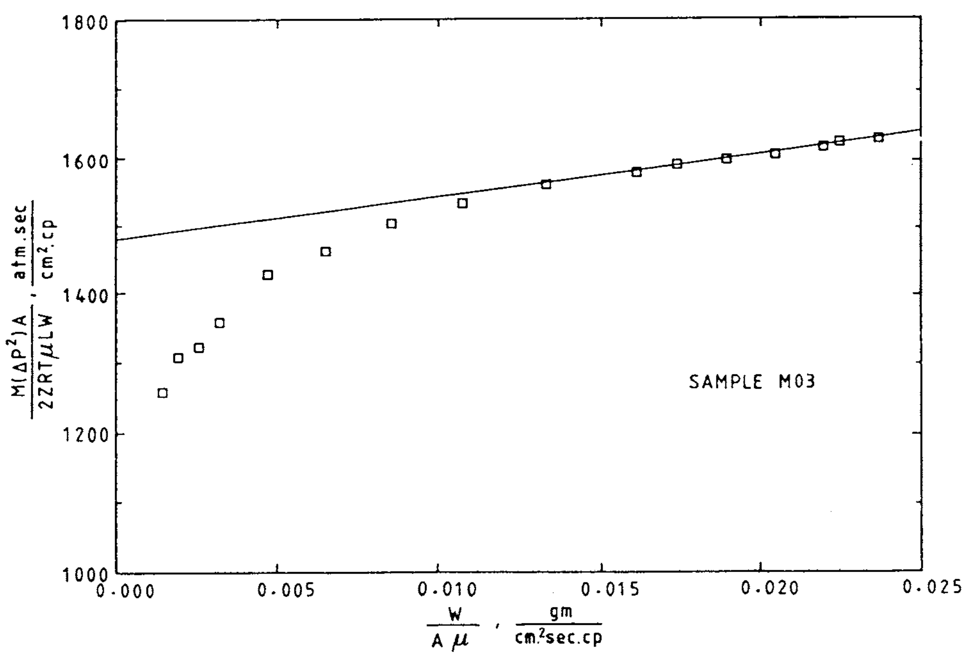

Fig. 2 An example of Forchheimer plot

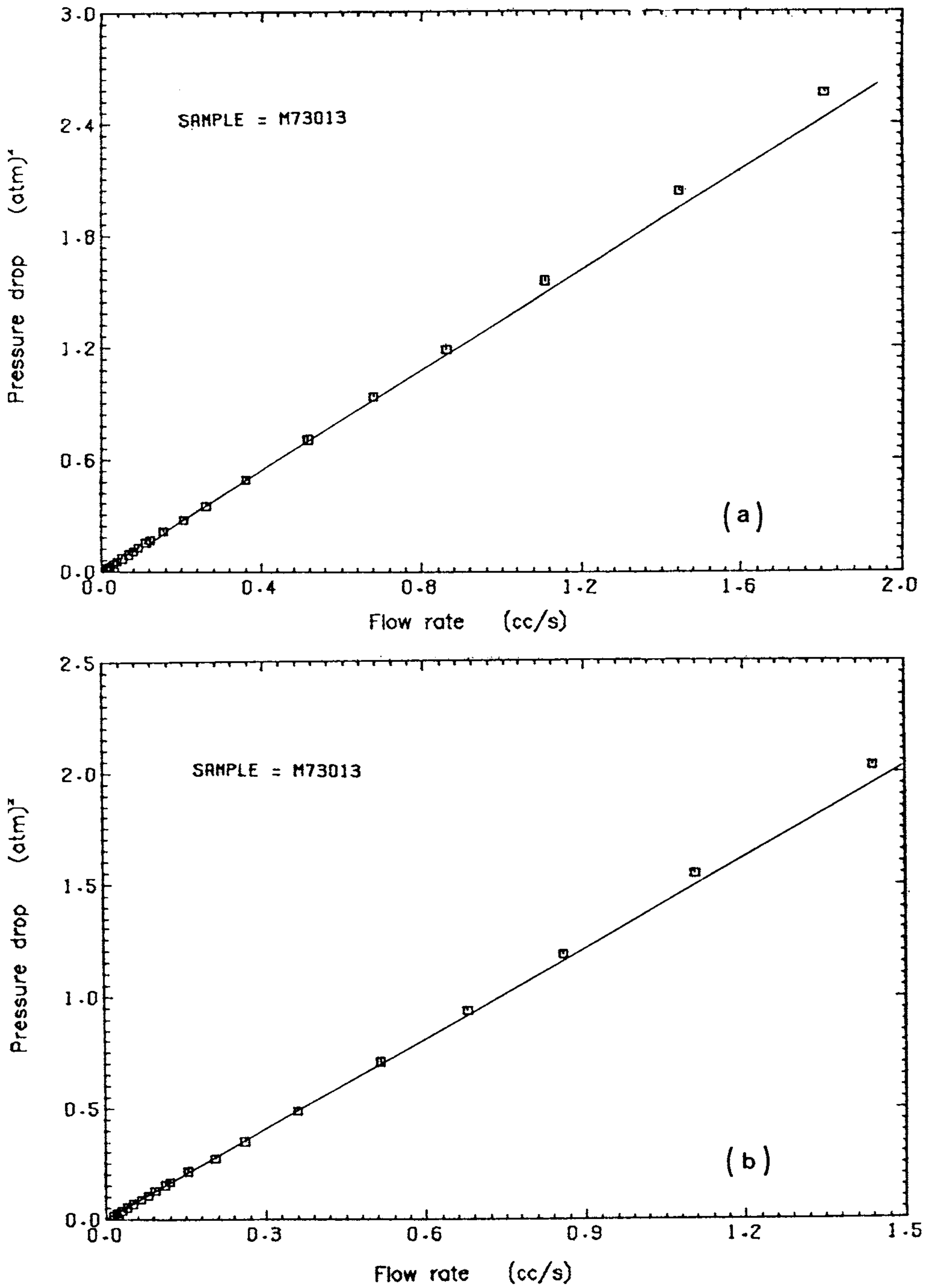

Fig. 3 (a) Pressure gradient (P_1^2-P_2^2) against flow rate.
(b) Enlarged view of the previous plot.

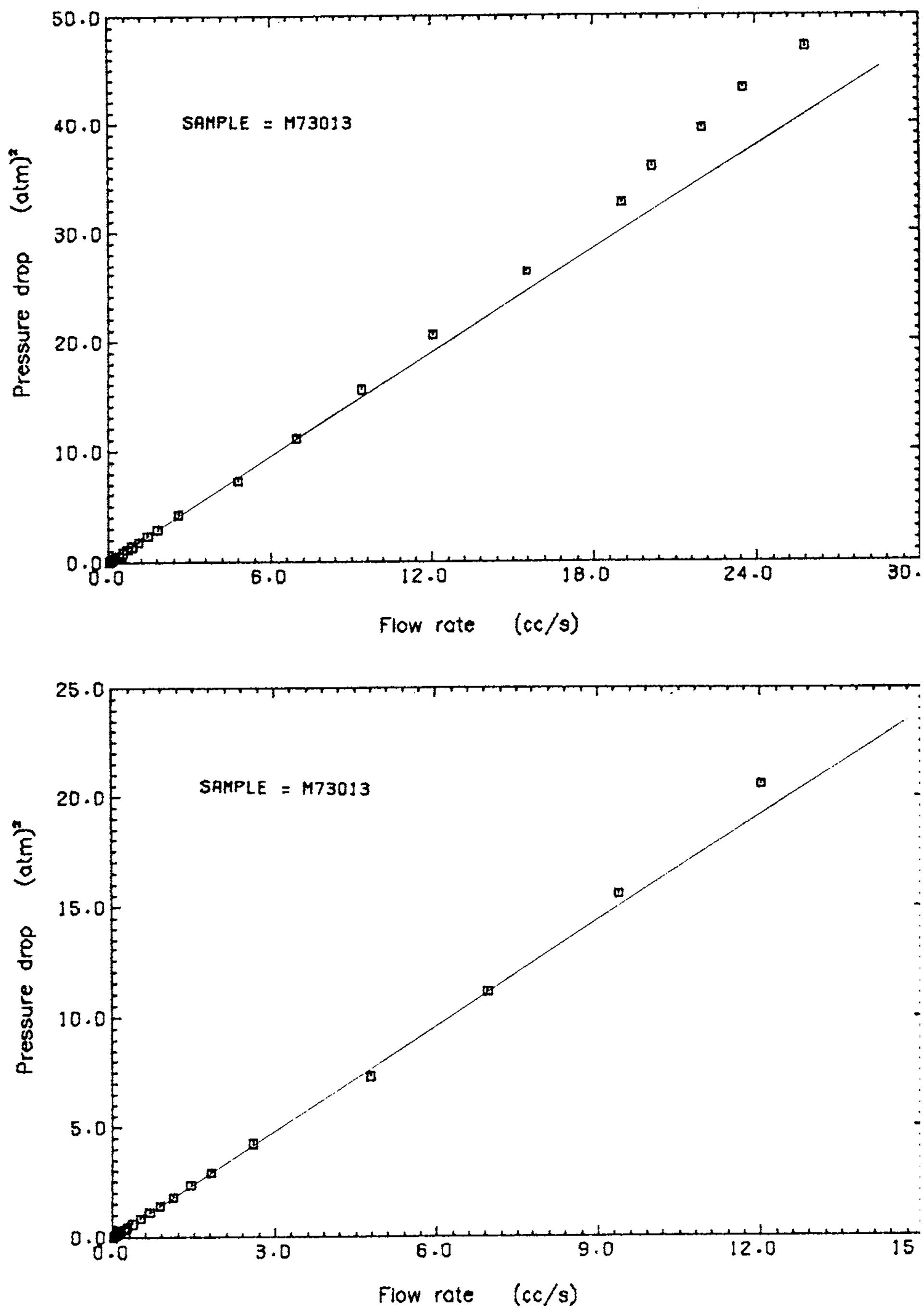

Fig. 4 (a) Modified pressure gradient to take account of slippage against flow rate. (b) Enlarged view of the plot.

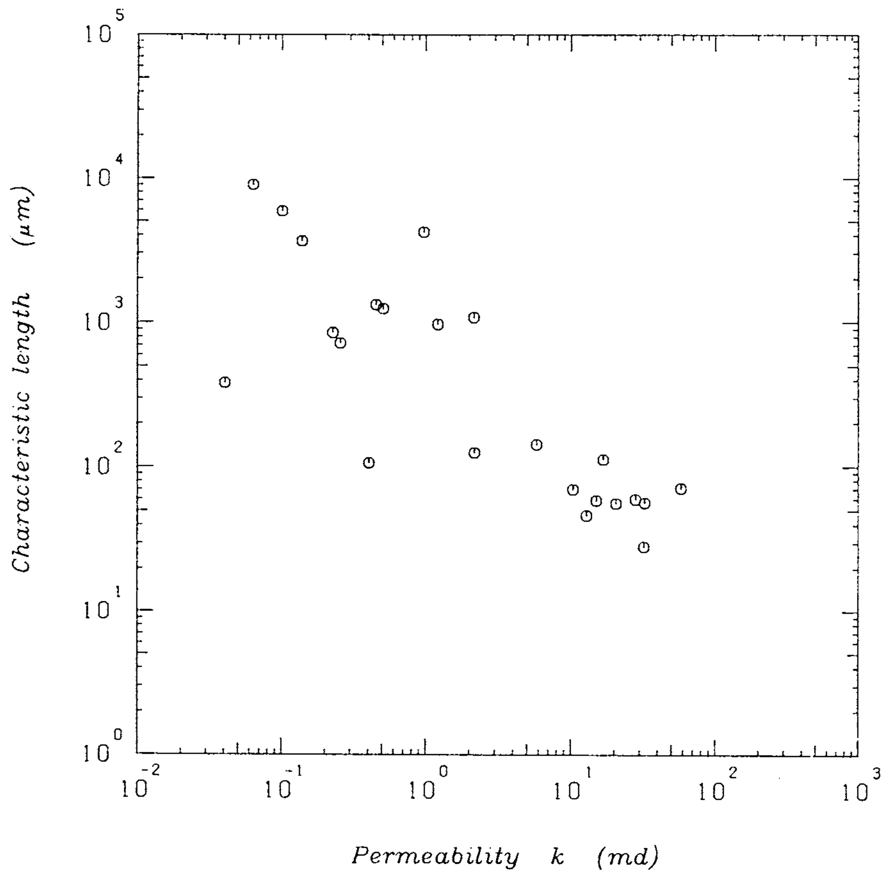

Fig. 5 Relationship between the characteristic length and permeability.

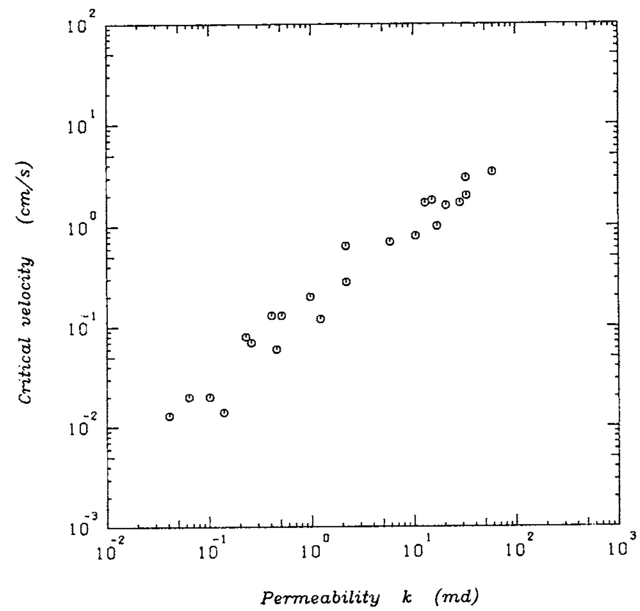

Fig. 6 Critical flow velocity at the onset of deviation from Darcy's law against permeability.

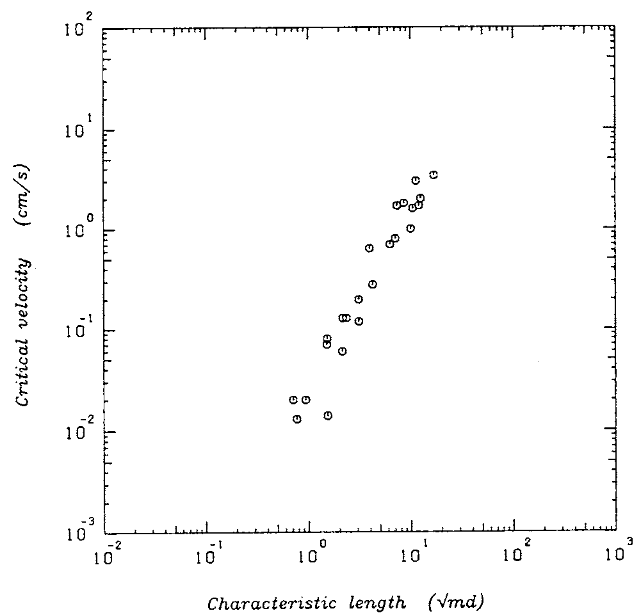

Fig. 7 Critical flow velocity against a characteristic length of the media $\sqrt{(k/\phi)}$.